Electronic Supplementary Material (ESI) for Dalton Transactions.

Electronic Supplementary Information

Simultaneous introduction of various palladium active sites into MOF *via* one-pot synthesis: Pd@$[Cu_{3-x}Pd_x(BTC)_2]_n$

Wenhua Zhang,[a] Zhihao Chen,[c] Majd Al-Naji,[c] Penghu Guo,[d] Stefan Cwik,[a] Olesia Halbherr,[a] Yuemin Wang,[e] Martin Muhler,[d] Nicole Wilde,[c] Roger Gläser[c] and Roland A. Fischer*[b]

Experimental Section

General procedure

All chemicals ($Cu(NO_3)_2 \cdot 3H_2O$, Pd acetate, $PdCl_2$, benzene-1,3,5-tricarboxylic acid (H_3BTC), *p*-nitrophenol (PNP) (99%), sodium borohydrate ($NaBH_4$) (98%)) and all solvents (H_2O, ethanol and acetone) were used as commercially received unless otherwise noted.

The Powder X-Ray diffraction (PXRD) data were performed on an X' Pert PRO PANalytical diffractometer(Bragg–Brentano geometry with automatical divergence slits, position sensitive detector, continuous mode, room temperature, Cu-Kα radiation, Ni-filter, in the range of 2Θ = 5–50°, step size 0.01°, time per step 250 s). FTIR spectra were recorded on a Bruker Alpha FTIR instrument in the ATR geometry with a diamond ATR unit in the range 400–4000 cm^{-1} inside a LABStar MB 10 compact MBraun glove-box (argon atmosphere). Liquid phase ^{1}H-NMR spectra were measured on a Bruker Avance DPX-200 spectrometer at 293 K in DCl/DMSO-d_6 for the digested activated MOF samples using TMS as internal standards and normalizing the signals to the DMSO-d_6 signal. N_2 sorption measurements were performed using a Quantachrome Autosorp-1 MP instrument, optimized protocols and N_2 of 99.9995% purity or a Micromeritics 3Flex instrument. Thermogravimetric analyses (TGA) were collected using a TG/DSC NETZSCH STA 409 PC instrument at a heating rate of 5 K min^{-1} in a temperature range from 30–600 °C (sample weight 5–10 mg) under N_2 (99.999%;) gas flow (20 ml min^{-1}). Atomic absorption spectroscopic (AAS) analysis to determine *Cu* and *Pd* contents were performed in the Microanalytical Laboratory of the Department of Analytical Chemistry at the Ruhr-University Bochum. An AAS apparatus by Vario of type 6 (1998) was employed. Scanning electron microscopy (SEM) and Energy-dispersive X-ray spectroscopy (EDX) images were recorded from an FEI ESEM Dual Beam™ Quanta 3D FEG microscope. X-ray photoelectron spectroscopy (XPS) measurements were performed in a UHV setup equipped with a high-resolution Gammadata-Scienta SES 2002 analyzer. A monochromatic Al Kα X-ray source (energy 1486.6 eV) was used as incident radiation. The analyzer slit width was set at 0.3 mm and the pass energy was fixed at 200 eV for all the measurements. The overall energy resolution was better than 0.5 eV. A flood gun was used to compensate for the charging effects. All spectra reported here are calibrated to the C 1s corelevel binding energy at 285 eV. The XP spectra were deconvoluted using the CASA XPS program with a mixed Gaussian–Lorentzian function and Shirley background subtraction.

Synthesis of $[Cu_3(BTC)_2]_n$ (Cu-BTC)

$[Cu_3(BTC)_2]_n$ was prepared following a reported method [1] at a little lower temperature (100 °C). Specifically, $Cu(NO_3)_2 \cdot 3H_2O$ (1.8 mmol, 438 mg) and H_3BTC (1.0 mmol, 210 mg) were put into a Teflon vessel, and 12 ml of H_2O:EtOH (1:1) solution was subsequently added. The vessel was sealed in an autoclave and kept in a preheated oven at 100 °C for 12 h. The observed crude product was filtered and washed several times with distilled water and absolute ethanol. After

drying under ambient conditions the obtained powder (152 mg) was further activated by heating at 120 °C for 24 h under dynamic vacuum (ca. 10^{-3} mbar).

Synthesis of Cu/Pd-BTC_1-3

For synthesis of **Cu/Pd-BTC_1-3**, 2.0 mmol of H_3BTC (420 mg) was combined with 1.8 molar equivalents of a mixture of $Cu(NO_3)_2{\cdot}3H_2O$ and Pd(II) acetate and then placed into a Teflon vessel. Subsequently 15ml of H_2O/ EtOH (1:1) solution was added. The molar percentage and amount of each metal salts in the total metal source as well as their weight used in the starting reaction mixture are: for **Cu/Pd-BTC_1** - $Cu(NO_3)_2{\cdot}3H_2O$ (90%, 3.24 mmol, 783 mg) / $Pd(OOCCH_3)_2$ (10%, 0.36 mmol. 80.8 mg); for **Cu/Pd-BTC_2** - $Cu(NO_3)_2{\cdot}3H_2O$ (85%, 3.06 mmol, 739 mg) / $Pd(OOCCH_3)_2$ (15%, 0.54 mmol. 121.2 mg); for **Cu/Pd-BTC_3** - $Cu(NO_3)_2{\cdot}3H_2O$ (80%, 2.88 mmol, 696 mg) / $Pd(OOCCH_3)_2$ (20%, 0.72 mmol. 161.6 mg). Afterwards the Teflon vessels were sealed in autoclaves and kept at 125 °C for 12h. The resulting powder product was collected by filtration and washed several times with distilled water and acetone. After drying under ambient conditions the obtained powder was activated by heating at 120 °C for 24 h under dynamic vacuum (ca. 10^{-3} mbar).

Synthesis of Cu/Pd-BTC_4

For sample **Cu/Pd-BTC_4**, 0.48 mmol of H_3btc (101 mg) was combined with 1.5 molar equivalents of mixture of $Cu(NO_3)_2{\cdot}3H_2O$ (80%, 0.58 mmol, 139 mg) / $PdCl_2$ (20%, 0.14 mmol. 25.5 mg) and then placed into a Teflon vessel. Subsequently 6ml of H_2O/ethanol (1:1) solution was added. The Teflon vessel was sealed in an autoclave and kept in the oven at 90 °C for 16h. The resulting power product was collected by filtration and washed several times with distilled water and acetone, respectively. After dried under ambient conditions the obtained powder was further activated by heating at 120 °C for 24 h under dynamic vacuum (ca. 10^{-3} mbar).

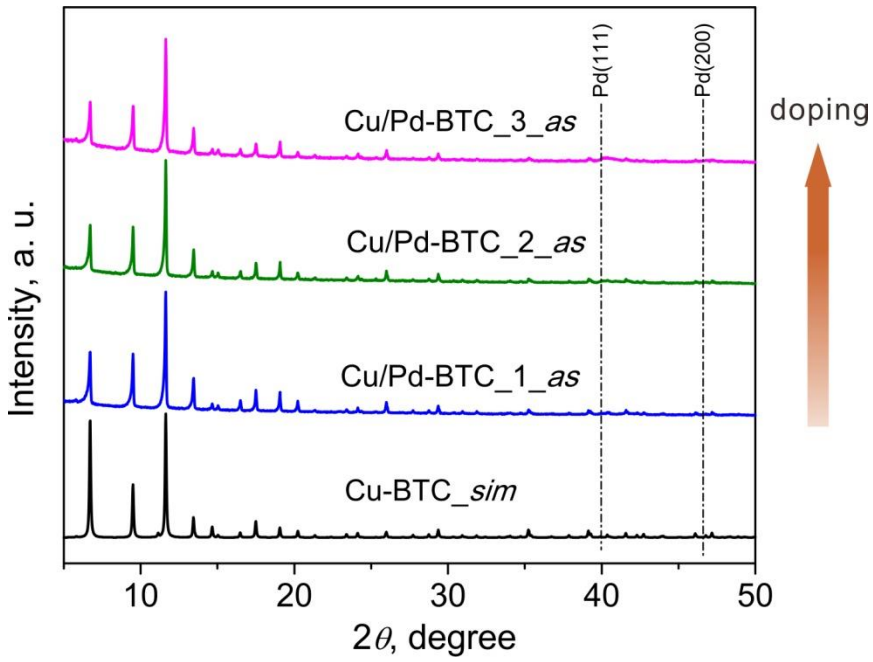

Figure S1. PXRD patterns of the as-synthesized Pd@$[Cu_{3-x}Pd_x(BTC)_2]_n$ (**Cu/Pd-BTC_1-3**) in comparison with simulated patterns of non-doped $[Cu_3(BTC)_2]_n$. The vertical dash lines correspond to the peak position of (111) and (200) planes of the face-centered cubic (fcc) Pd-structure.

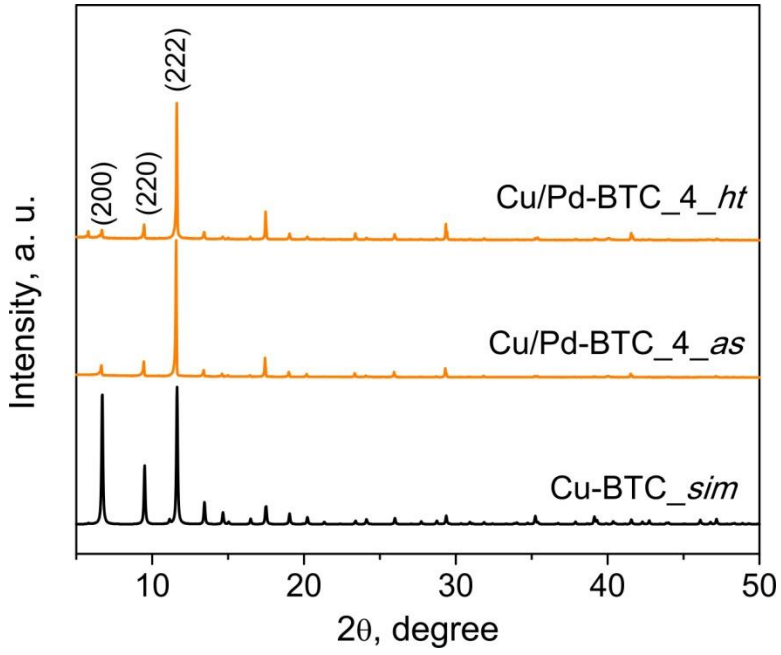

Figure S2. PXRD patterns of the as-synthesized and activated **Cu/Pd-BTC_4** in comparison with simulated patterns of non-doped $[Cu_3(BTC)_2]_n$ (Cu-BTC_*sim*). The well matched patterns with parent Cu-BTC suggest that the crystallinity of **Cu/Pd-BTC_4** is preserved after the doping of Pd-species.

Table S1. Calculated cell parameters of the **Cu/Pd-BTC_1-3** (TOPAS academic software and Pawley method[2] has been employed) in comparison with that obtained from the single crystal data of the reported $[Cu_3(BTC)_2]_n$.

Sample	a (Å)	V (Å^3)	Space group	R_{wp}	R_{exp}
$[Cu_3(BTC)_2]_n$[1]	26.343	18280	Fm-3m	-	-
Cu/Pd-BTC_1	26.308	18208	Fm-3m	6.018	4.79
Cu/Pd-BTC_2	26.305	18203	Fm-3m	6.618	5.17
Cu/Pd-BTC_3	26.293	18178	Fm-3m	7.201	6.09

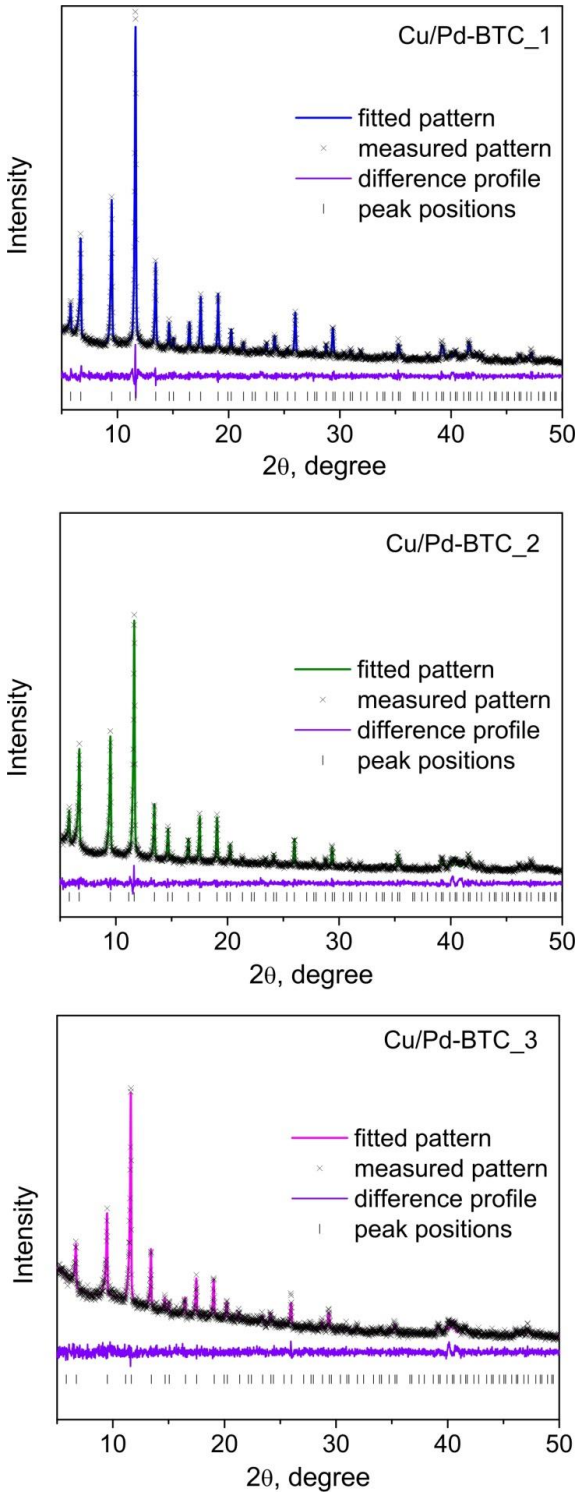

Figure S3. Pawley Fits of samples **Cu/Pd-BTC_1-3**. Blue, olive and magenta lines represent the fitted pattern of **Cu/Pd-BTC_1, 2** and **3**, respectively. Black ticks - theoretical positions of the Bragg reflections; Black crosses - the experimental data; Violet lines - the difference between fitted and measured patterns.

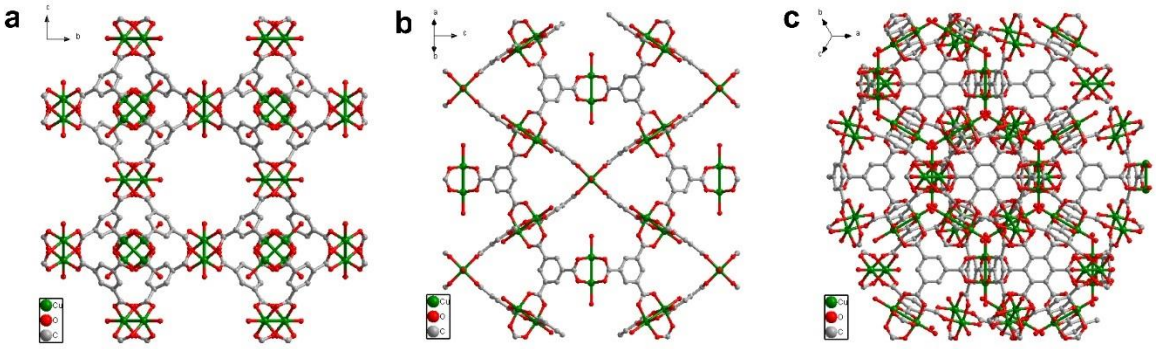

Figure S4. Crystal structure of Cu-HKSUT-1 (**$[Cu_3(BTC)_2]_n$**) viewing along plane (200) (a), plane (220) (b)and plane (222) (c).

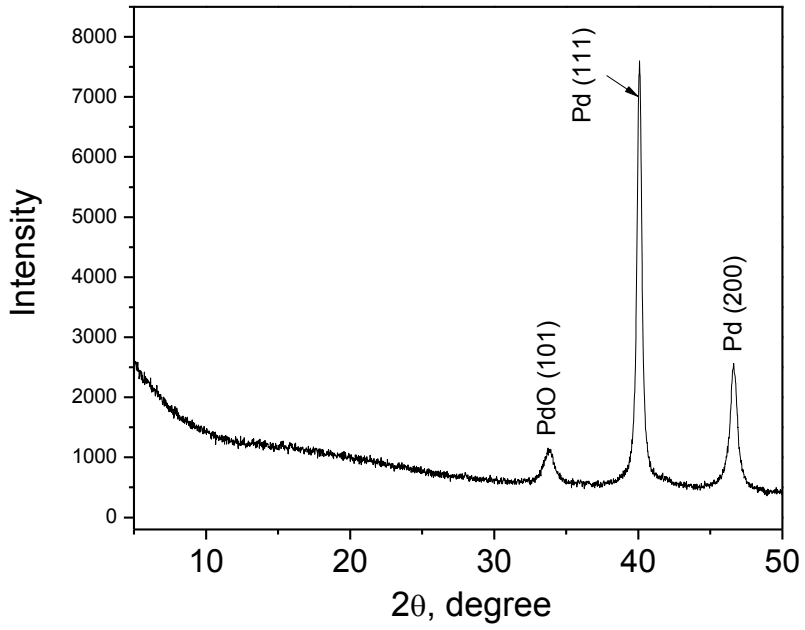

Figure S5. PXRD patterns of the sample prepared using only Pd(II)-acetate and H_3BTC under the same conditions as introduced mixed-metal solids with 10%, 15% and 20% feeding of Pd(II)-acetate. No Cu-salt was employed.

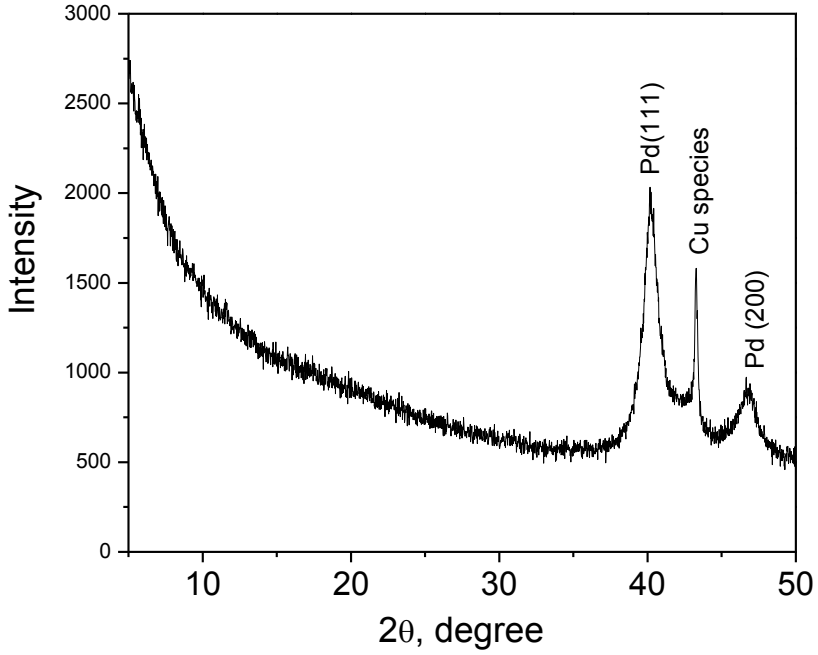

Figure S6. PXRD patterns of the sample obtained using 50% feeding of Pd(II)-acetate under the same conditions as Pd@$[Cu_{3-x}Pd_x(BTC)_2]_n$ with 10%, 15% and 20% feeding .

Table S2. Feeding and obtained contents of Pd in respect to the total metal amount in Pd@$[Cu_{3-x}Pd_x(BTC)_2]_n$ **(Cu/Pd-BTC_1-4)**. The Pd-molar fraction(%) were calculated from the obtained AAS results.

Sample	feeding (molar%)	obtained (molar%)	obtained wt%
Cu/Pd-BTC_1	10	9	3.9
Cu/Pd-BTC_2	15	14	6.2
Cu/Pd-BTC_3	20	20	9.2
Cu/Pd-BTC_4	20	12	5.2

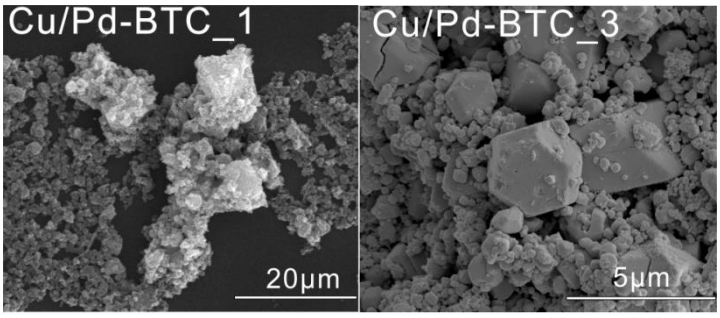

Figure S7. SEM images of samples **Cu/Pd-BTC_1** and **3.**

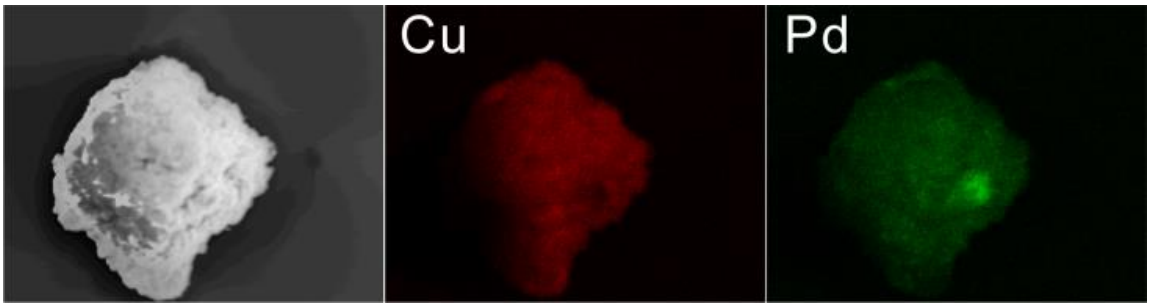

Figure S8. EDX elemental mapping of the **Cu/Pd-BTC_3** solid (red – Cu; green – Pd).

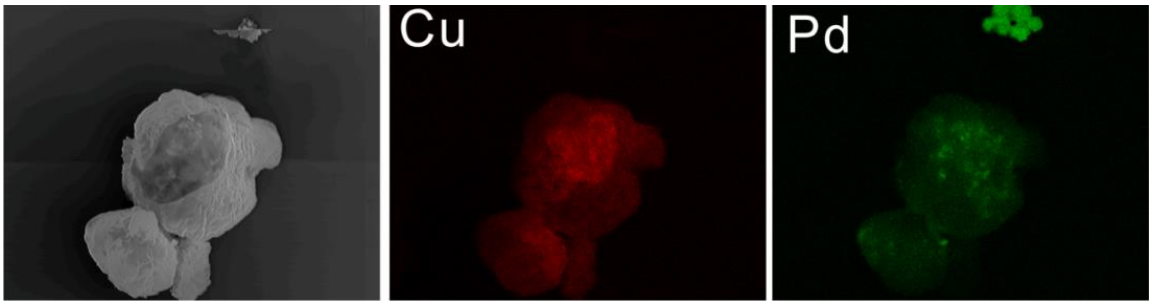

Figure S9. EDX elemental mapping of **Cu/Pd-BTC_4** which indicates the homogeneous distribution of Cu and Pd within the sample. Red: Cu mapping; green, Pd mapping.

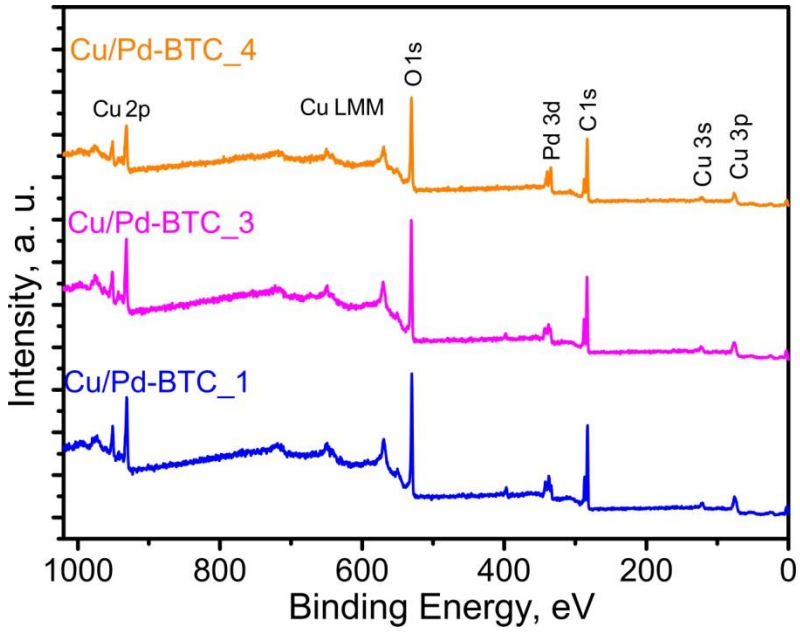

Figure S10. XPS survey scans of the obtained samples **Cu/Pd-BTC_1, _3** and **-4**. No detection of Cl indicates that Pd^{2+} in **Cu/Pd-BTC_4** should originate from Pd^{2+} framework incorporation rather than residual or loading $PdCl_2$.

Table S3. The assignment of binding energies as well as the determined molar fraction of Pd^{2+} and Pd^0 in **Cu/Pd-BTC_1, _3** and **_4**.

Sample	Binding energy, eV		Assignment	Molar fraction (%)	
	Pd $3d_{3/2}$	Pd $3d_{5/2}$		Pd^{2+}: (Pd^{2+} +Pd^0)	Pd^0: (Pd^{2+} +Pd^0)
Cu/Pd-BTC_1	344.2	338.9	Pd^{2+} (Pd1)	67	33
	343.2	337.9	Pd^{2+} (Pd2)		
	340.9	335.6	Pd^0 (Pd3)		
Cu/Pd-BTC_3	344.2	338.9	Pd^{2+} (Pd1)	56	44
	343.2	337.9	Pd^{2+} (Pd2)		
	341.2	335.9	Pd^0 (Pd3)		
Cu/Pd-BTC_4	343.6	338.4	Pd^{2+} (Pd1)	30	70
	342.4	337.2	Pd^{2+} (Pd2)		
	340.9	335.7	Pd^0 (Pd3)		

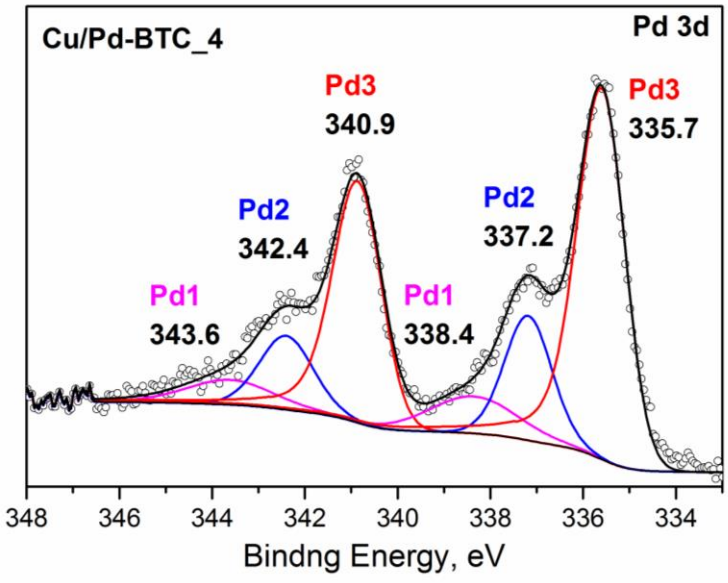

Figure S11. Deconvoluted XP spectra of **Cu/Pd-BTC_4** in Pd 3d region. The doublet with the label of Pd3 is attributed to the metallic Pd^0 species.

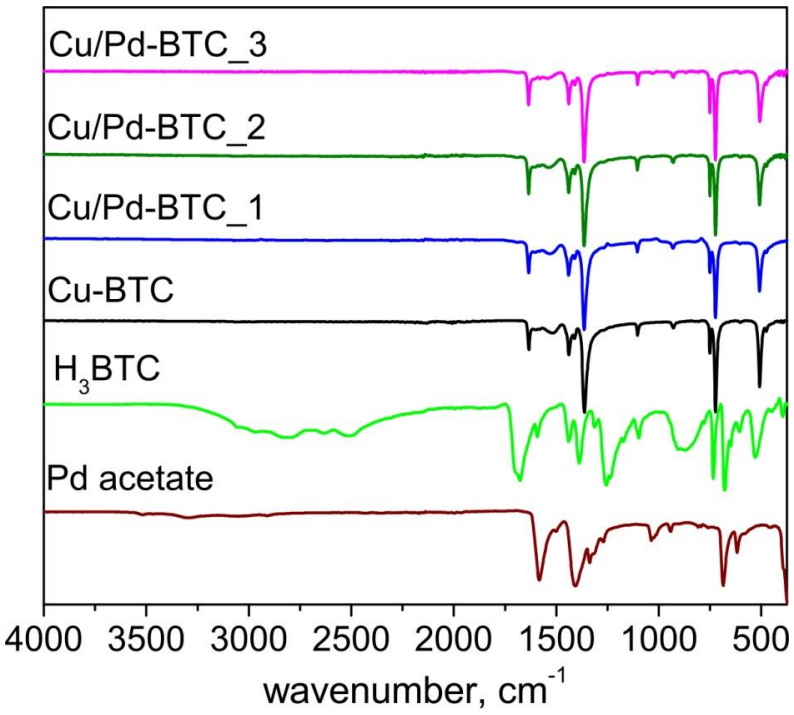

Figure S12. IR spectra of the activated samples **Cu/Pd-BTC_1-3** in comparison with parent Cu-BTC as well as H_3BTC and Pd-acetate.

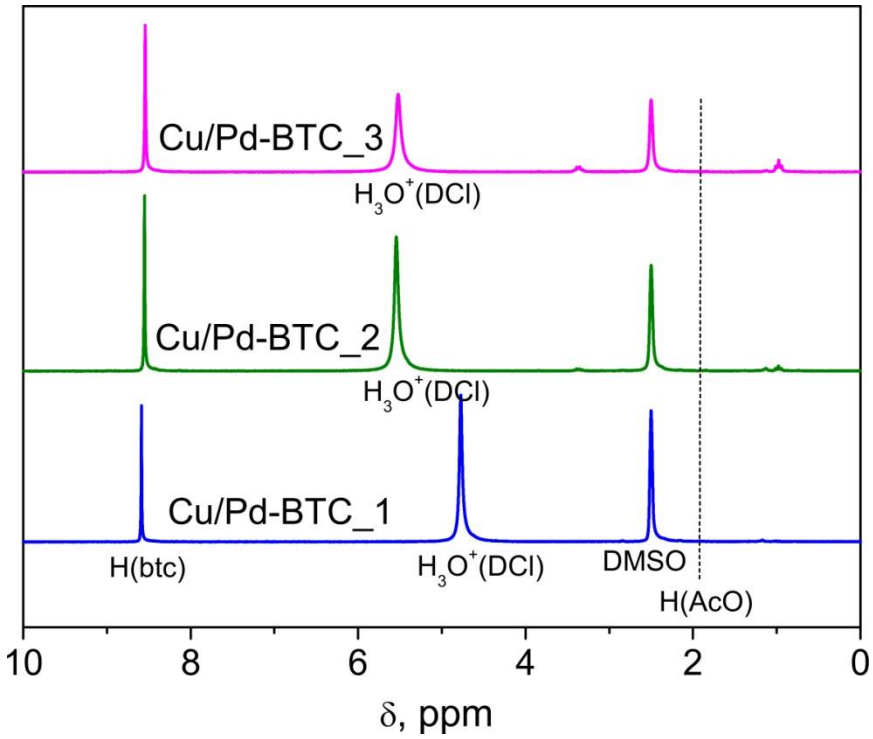

Figure S13. ^{1}H-NMR spectra of the digested activated **Cu/Pd-BTC_1-3** samples**.** The vertical dash line stands for the position where the peak of CH_3-protons from the acetic acid commonly appear.

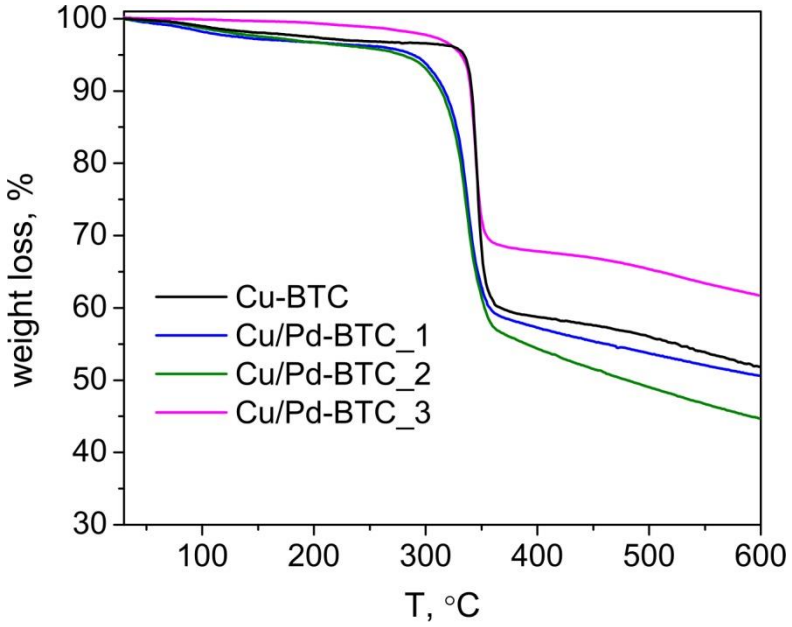

Figure S14. TG curves of the prepared Pd-doped solids **Cu/Pd-BTC_1-3** in comparison with "non-doped" material Cu-BTC.

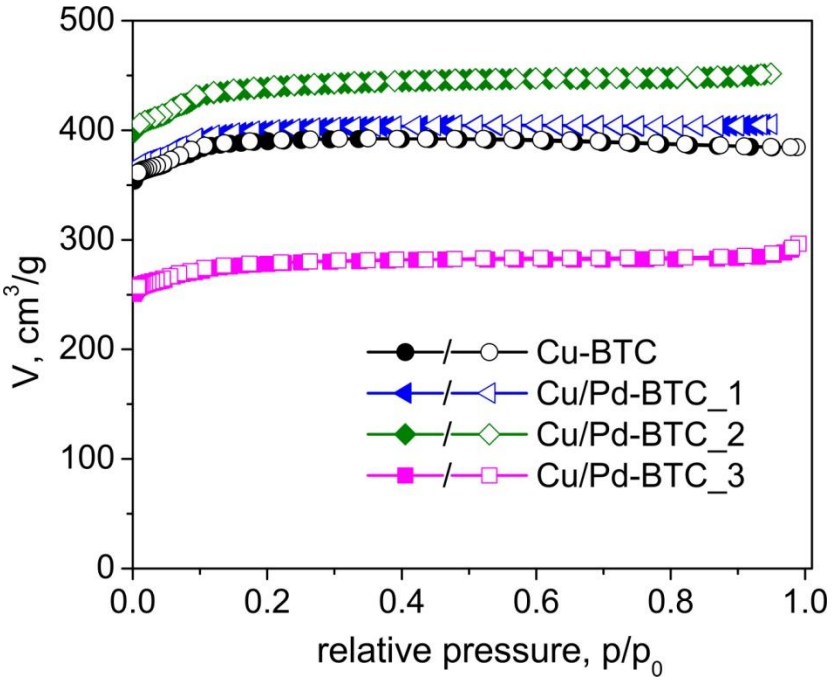

Figure S15. N_2 sorption isotherms collected at 77 K for the non-doped $[Cu_3(BTC)_2]_n$ (Cu-BTC) and Pd-doped solids $Pd@[Cu_{3-x}Pd_x(BTC)_2]_n$ (**Cu/Pd-BTC_1-3**).

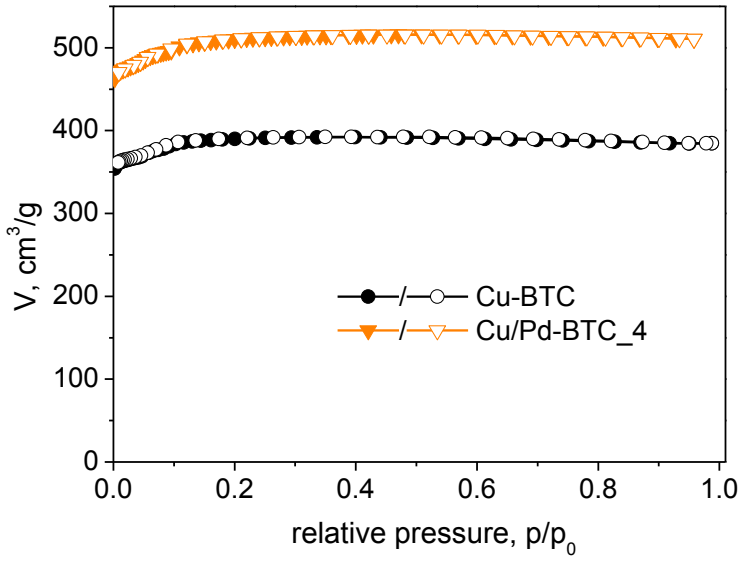

Figure S16. N_2 sorption isotherms collected at 77 K for the non-doped $[Cu_3(BTC)_2]_n$ (Cu-BTC) and Pd-doped solid **Cu/Pd-BTC_4**. The high surface area indicates the external Pd^0 particles rather than being included into the volumes of MOF.

Table S4. BET surface areas (S_{BET})* of **Cu/Pd-BTC_1-4** in comparison with "non-doped" Cu-BTC

Sample	S_{BET}(m^2/g)	S_{BET} (m^2/mmol)
Cu-BTC	1561	944
Cu/Pd-BTC_1 (9 mol% of Pd)	1594	982
Cu/Pd-BTC_2 (14 mol% of Pd)	1750	1090
Cu/Pd-BTC_3 (20 mol% of Pd)	1112	700
Cu/Pd-BTC_4 (12% of Pd)	2000	1240

* S_{BET} in the unit of m^2/g is calculated from the slope of BET plot by the software connected with the N_2 sorption instrument. S_{BET} in m^2/mmol unit is calculated from S_{BET}(m^2/g) and the estimated molecular weight. Specifically, the general formula of $Pd^0@[Cu_{3-x}Pd_x(BTC)_2]_n$ was concluded from two major data:

(i) The measured PXRD patterns of Cu/Pd_BTC is well-matched and fitted with the patterns of $[Cu_3(BTC)_2]_n$.

(ii) The presence of Pd^0 is determined from XPS and the small reflections at 40.02° in PXRD patterns.

Subsequently, the molar fraction of both Cu and Pd is calculated from the AAS results (mass fractions). Moreover, XPS results afford us the respective (relative) molar fraction of Pd^0 and Pd^{2+}. However, given that the quantitative determination of metal species from XPS is not as precise as AAS, we calculate the molar weight in a simpler way. Namely, the molar weight of Cu/Pd-BTC are determined on the basis of a formula of $[Cu_{3-x}Pd_x(BTC)_2]_n$ since the whole Pd content (including Pd^0 and Pd^{2+}) for each sample is the same no matter we treat it as $[Cu_{3-x}Pd_x(BTC)_2]_n$ or $Pd^0@[Cu_{3-x}Pd_x(BTC)_2]_n$. The tiny deviation of Cu content is omitted for simplification. Hence, assuming that all the solids are fully activated (*i.e.* no guest molecules occluded in the pores) before N_2 sorption analysis, the BET surface area per mole is then calculated from S_{BET}(m^2/g) and the estimate value of molecule weight for each sample: **Cu/Pd-**

BTC_1, $[Cu_{2.73}Pd_{0.27}(c_9h_3o_6)_2]_n$-616 g/mol; **Cu/Pd-BTC_2,** $[Cu_{2.58}Pd_{0.42}(c_9h_3o_6)_2]_n$-623 g/mol; **Cu/Pd-BTC_3**, $[Cu_{2.4}Pd_{0.6}(BTC)_2]_n$-630 g/mol; **Cu/Pd-BTC_4**, $[Cu_{2.64}Pd_{0.36}(btc)_2]_n$ -620 g/mol; **Cu-BTC**, $[Cu_3(btc)_2]_n$-605 g/mol.

Catalytic test reaction

The catalytic hydrogenation of PNP to PAP using $NaBH_4$ as a reducing agent was carried out in the aqueous phase using a 100 cm^3 batch reactor at room temperature (298K), ambient pressure and 1300 min^{-1} stirring speed.[3] In a typical catalytic experiment, 5.0 cm^3 of an aqueous solution of $NaBH_4$ (0.60 mmol dm^{-3}) were added to 90.0 cm^3 of an aqueous solution of PNP (0.18 mmol dm^{-3}). The reaction was started by introducing 5.0 mg of the activated catalyst (see "general procedure"). The PNP concentration changes was monitored *via* on-line UV-vis spectroscopy (AvaSpec-3648, optical path length: 5 mm) at a wavelength of 400 nm. The initial reaction rate (r_0) was calculated by assuming a zero order reaction from the linear decrease of PNP concentration after the addition of the catalyst.

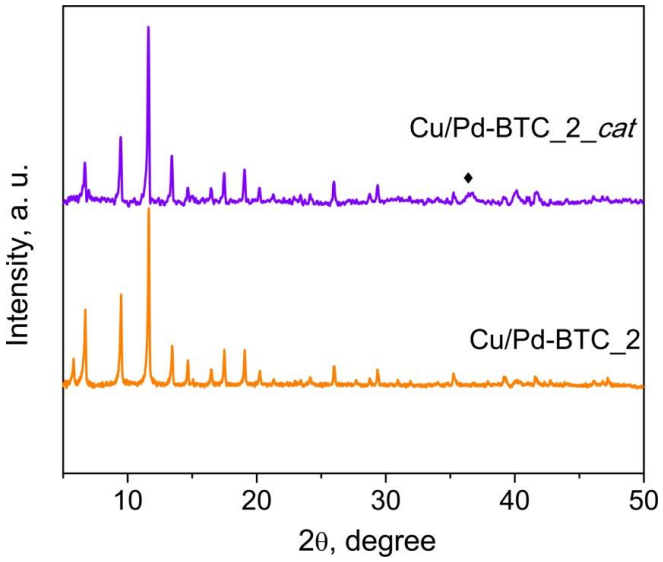

Figure S17. XPRD patterns of the sample with 14% of Pd-doping after the hydrogenation of PNP to PAP (**Cu/Pd-BTC_2_*cat***) in comparison with that before the reaction (**Cu/Pd-BTC_2**). The diamond symbol represents the reflection position of Cu_2O attributed to the reduction by $NaBH_4$.

References

1. S. S. Y. Chui, S. M. F. Lo, J. P. H. Charmant, A. G. Orpen and I. D. Williams, *Science*, 1999, **283**, 1148-1150.

2. G. Pawley, *J. Appl. Cryst.*, 1981, **14**, 357-361.

3. M. Goepel, M. Al-Naji, P. With, G. Wagner, O. Oeckler, D. Enke and R. Gläser, Chem. Eng. Technol., 2014, 37, 551-554.